Focusing problem in radio tomography

V.P. Yakubov, S.A. Slavgorodskii, and V.P. Kutov

Tomsk State University

Received June 4, 2003

Results of theoretical and experimental research on development of the radio tomography method are presented. An emphasis is on the problem of localization of radiation interaction with a medium. Combined use of the physical and mathematical focusing is proposed for solution of the problem. High efficiency of the proposed approach for inhomogeneous medium tomography is demonstrated experimentally with the use of two sensing schemes: in transmitted and reflected light, as well as multiposition and multifrequency sensing. About 1 cm resolution is achieved for test and real inhomogeneities.

Introduction

Radio tomograph is a device employing electromagnetic radiation in the radio region to retrieve the internal electrophysical structure of the object under study based on results of radio sensing. The method of radio tomography extends the range of measurable parameters and well complements the well-known methods of X-ray, NMR, and ultrasonic tomography.[1–3]

Tomographic systems for diagnostics of inhomogeneous media are now finding increasing use in different fields of industry and research. The most intense development of such systems is observed in medicine. Traditional tomographic scanning systems based on X-ray radiation have a destructive effect on biological media and do not resolve low-contrast inhomogeneities. Thus, development of new, ecologically safe systems for visualization of the internal structure of sensed media seems to be urgent.

From this point of view, the radio tomography methods are most promising, because the use of electromagnetic radiation of the radio range permits one to extract much more information from tomography of various media due to high sensitivity of radio waves to small variations of permittivity. However, practical realization of radio tomographic methods faces some difficulties.

The first difficulty is the diffraction and multiple interaction of radiation with the sensed medium, where the wavelength is comparable with the size of inhomogeneities.

The second difficulty is connected with the fact that real media can screen and absorb electromagnetic waves. Thus, one of the first problems in radio tomography is to take into account the multiple interaction of radiation with inhomogeneities of an object through either adequate description of inhomogeneities or instrumental removal of their effect.

In this paper, we consider the radio tomograph realization based on localization of radiation interaction with the matter through focusing, which significantly decreases the effect of diffraction and multiple interactions and thus improves the accuracy in interpretation of sensing results.

Two sensing schemes are considered. The *first* one uses the transmitted light, when the source and the receiver of radiation are located on different sides of the sensed volume and radiation passes through all inhomogeneities. This scheme is traditional in tomography. A novelty is in the use of radio radiation. The *second* scheme utilizes the reflected light, when the source and the receiver are in one half-space, while the sensed volume is in another one. We consider the most general case of antennas separated by some distance from the sensed volume, that is, when direct contact with a medium is absent or impossible by some reasons. Such a situation takes place, for example, when detecting plastic mines in soil or when sensing open wounds. Both schemes under consideration imply the multiposition and multifrequency sensing with focusing.

1. Mathematical and physical focusing of radiation

Consider first the mathematical model of formation of wave projections in the case of the transmission sensing scheme, that is, in transmitted light. For the illuminating wave field in the focal zone (Fig. 1) we can write the following equation:

$$E_0(\mathbf{r}_0) = \iint\limits_{S_1} I(\mathbf{r}_F, \mathbf{r}_1) G^{(+)}(\mathbf{r}_1, \mathbf{r}_0) \mathrm{d}s_1,$$

where

$$G^{(+)}(\mathbf{r}_1, \mathbf{r}_0) = \exp\{ik|\mathbf{r}_1 - \mathbf{r}_0|\}/4\pi|\mathbf{r}_1 - \mathbf{r}_0|$$

is the Green's function, $k = 2\pi/\lambda$ is the wave number, and $I(\mathbf{r}_F, \mathbf{r}_1)$ is the current on the surface of the emitting aperture S_1. The amplitude–phase distribution of this current should provide for radiation focusing at the point $\mathbf{r}_F$. According to the double focusing method, this distribution is described by the equation[4,5]:

$$I(\mathbf{r}_F, \mathbf{r}_1) = \frac{1}{4i\pi^2} \frac{\mathrm{d}}{\mathrm{d}n_1} G^{(-)}(\mathbf{r}_F, \mathbf{r}_1).$$

Here

$$G^{(-)}(\mathbf{r}_F, \mathbf{r}_1) = \exp\{-ik|\mathbf{r}_F - \mathbf{r}_1|\}/4\pi|\mathbf{r}_F - \mathbf{r}_1|$$

is the Green's function of the inverse wave field. The use of the function $I(\mathbf{r}_F, \mathbf{r}_1)$ leads to inphase addition of waves near the focal point.

0235-6880/03/09 746-04 $02.00

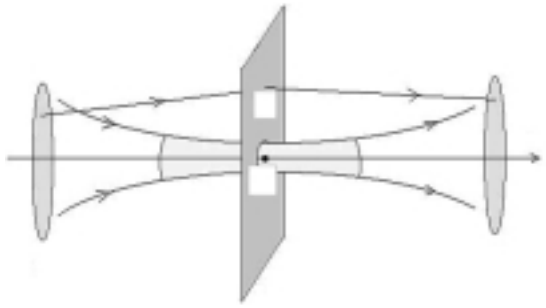

Fig. 1. Focusing system.

The field of the illuminating wave $E_0(\mathbf{r}_0)$ interacts with the propagation medium. The main mechanism of this interaction is the diffraction at inhomogeneities of the refractive index $\Delta n(\mathbf{r}_0) = n - 1$. In the general case, this function is complex. To describe mathematically the arising complex phenomenon, different approximate methods are used. In our opinion, the most simple and adequate method for the problem at hand is based on the so-called phase approximation of the Huygens–Kirchhoff method.[6] The method is widely used for description of strong fluctuations in turbulent media. According to this method, the diffraction field is described by the integral

$$E(\mathbf{r}_2) = \iint\limits_{S_0} E_0(\mathbf{r}_0) \frac{\mathrm{d}}{\mathrm{d}z_0} G^{(+)}(\mathbf{r}_2, \mathbf{r}_0) \exp\left\{ik \int \Delta n\left(\mathbf{r}_0'\right) \mathrm{d}z'\right\} \mathrm{d}s_0.$$

Here S_0 is the virtual Huygens plane drawn across the working wave zone near the focal plane (see Fig. 1). Integration over z' in the exponent accounts for the additional phase shift caused by inhomogeneities along the straight line connecting the current point on the Huygens plane $\mathbf{r}_0$ and the point $\mathbf{r}_2$ in the reception plane S_2. Such geometric-optic description, in spite of its simplicity, nevertheless allows a good description of diffraction in inhomogeneous media.

The field of the wave having passed through the sensing object focuses again on the plane S_2. The signal recorded in this case is described by the integral

$$E_2(\mathbf{r}_F) = \iint\limits_{S_2} I(\mathbf{r}_F, \mathbf{r}_2) E(\mathbf{r}_2) \mathrm{d}s_2$$

or

$$E_2(\mathbf{r}_F) = \iint\limits_{S_0} Q(\mathbf{r}_F, \mathbf{r}_0) f(\boldsymbol{\rho}_0) \mathrm{d}s_0, \qquad (1)$$

where the refractive index perturbation is included through the function

$$f(\boldsymbol{\rho}_0) = \exp\left\{ik \int \Delta n\left(\mathbf{r}_0'\right) \mathrm{d}z'\right\}$$

and

$$Q(\mathbf{r}_F, \mathbf{r}_0) = \iint\limits_{S_1} I(\mathbf{r}_F, \mathbf{r}_1) G^{(+)}(\mathbf{r}_1, \mathbf{r}_0) \mathrm{d}s_1 \iint\limits_{S_2} I(\mathbf{r}_F, \mathbf{r}_2) \frac{\mathrm{d}}{\mathrm{d}z_0} G^{(+)}(\mathbf{r}_2, \mathbf{r}_0) \mathrm{d}s_2 \qquad (2)$$

denotes the instrumental function of the focusing system.

If the focusing point $\mathbf{r}_F$ is located on the axis just in the middle between the focusing apertures S_1 and S_2, then the instrumental function $Q(\mathbf{r}_F, \mathbf{r}_0)$ has the axial symmetry and the form of a body of revolution. The calculation conducted, for example, for radiation with the working wavelength $\lambda = 2\pi/k =$ = 3 cm has shown that the localization area of the function $Q(\mathbf{r}_F, \mathbf{r}_0)$ at the half-power level has the longitudinal size of about 30 cm with the cross size of 3 cm. In the chosen approximation, the localization area is independent of the medium parameters, and with the given arrangement of the transmitting and receiving apertures it is determined only by the mutual arrangement of the points $\mathbf{r}_F = (x_F, y_F, z_F)$ and $\mathbf{r}_0 = (x_0, y_0, z_0)$ and the wavelength λ. Taking this into account, we can assume that

$$Q(\mathbf{r}_F, \mathbf{r}_0) = Q(\boldsymbol{\rho}_F - \boldsymbol{\rho}_0, z_0),$$

where z_0 describes the position of the virtual Huygens plane S_0, $\boldsymbol{\rho}_F = (x_F, y_F)$, $\boldsymbol{\rho}_0 = (x_0, y_0)$. In this case, the integral (1) has the form of convolution and describes the wave spread of geometric-optics projections of the object under study.

The information on the distribution of perturbations of the refractive index $\Delta n(\boldsymbol{\rho}_0, z_0)$ is contained in the function $f(\boldsymbol{\rho}_0)$. If we separate the contributions to the signal connected only with medium perturbations, then in place of Eq. (1) we can write

$$\Delta E_2(\mathbf{r}_F) = \iint\limits_{S_0} Q(\mathbf{r}_F, \mathbf{r}_0) \Delta f(\boldsymbol{\rho}_0) \mathrm{d}s_0, \qquad (3)$$

where

$$\Delta f(\boldsymbol{\rho}_0) \equiv f(\boldsymbol{\rho}_0) - 1 = \exp\left\{ik \int \Delta n\left(\mathbf{r}_0'\right) \mathrm{d}z'\right\} - 1.$$

The complete set of all possible wave projections of the object under study contains the full information on the spatial distribution of its electrophysical properties, that is, allows retrieval of the function $\Delta n(\boldsymbol{\rho}_0, z_0)$.

In the case of multifrequency or pulsed sensing, it is sufficient to pass on in Eq. (2) into the time domain using the Fourier transform. The arising instrumental function – a pulsed characteristic of the system – is calculated as

$$\hat{Q}(\boldsymbol{\rho}_0; z_0; t) = \frac{1}{2\pi} \int\limits_{-\infty}^{\infty} Q(\boldsymbol{\rho}_0, z_0; k = \frac{\omega}{c}) E_0(\omega) \exp\{-i\omega t\} \mathrm{d}\omega.$$

Here

$$E_0(\omega) = \int\limits_{-\infty}^{\infty} E_0(t) \exp\{i\omega t\} \mathrm{d}t$$

is the spectrum of the sensing signal. When using a broad band of sensing frequencies, the pulsed characteristic is well localized in time and, consequently, in the longitudinal coordinate $z = tc$.

If we use the lidar sensing scheme, in which the receiving aperture S_2 is integrated with the transmitting aperture S_1, then only the contribution

connected with medium perturbations is recorded and Eq. (3) is applicable. If in this case the transmitting and receiving antennas are interconnected, for example, are located at a fixed distance **d** and during spatial scanning in the plane $S_1 = S_2$ move simultaneously so that always $\mathbf{r}_2 = \mathbf{r}_1 + \mathbf{d}$, then in Eq. (2) we should replace

$$I(\mathbf{r}_F, \mathbf{r}_2) \to I(\mathbf{r}_F, \mathbf{r}_2)\delta(\boldsymbol{\rho}_2 - \boldsymbol{\rho}_1 - \mathbf{d}).$$

As a result, one surface integral in Eq. (2) is removed, and the equation for the instrumental function becomes much more simple:

$$Q(\mathbf{r}_F, \mathbf{r}_0) = \iint_{S_1} I(\mathbf{r}_F, \mathbf{r}_1) I(\mathbf{r}_F, \mathbf{r}_1 + \mathbf{d}) G^{(+)}(\mathbf{r}_1, \mathbf{r}_0) \frac{\mathrm{d}}{\mathrm{d}z_0} \times$$

$$\times G^{(+)}(\mathbf{r}_2 = \mathbf{r}_1 + \mathbf{d}, \mathbf{r}_0)\, \mathrm{d}s_1. \qquad (4)$$

The corresponding pulsed characteristic of the system $\hat{Q}(\boldsymbol{\rho}_0; z_0; t = 2z_0/c)$ at the wide spectrum of the sensing signal and large size of the aperture becomes sufficiently well localized in the 3D space. In this case, localization in the cross coordinates is achieved due to focusing and synthesizing the aperture, while in the longitudinal coordinate z_0 it is achieved due to pulsed scanning.

The proposed focusing algorithm is simple enough and can be realized through the spatial scanning with the use of the near-omnidirectional transmitting and receiving antennas. This operation is called aperture synthesizing. In this case, the focusing is a purely mathematical operation realized in a computer. The scanning can be replaced by a serial poll of a multielement antenna array. This corresponds to the use of the so-called distributed aperture. In this case, integrals in Eqs. (2) and (4) can be calculated both mathematically on the computer and instrumentally (at the physical level) using integral elements: cables, multichannel integrators, etc. The easiest instrumental realization can be obtained using the traditional focusing elements: mirrors and lenses. But in spite of simplicity, this method has some disadvantages, namely, the need of using a mechanical system for spatial scanning and impossibility of real-time correction of frequency distortions in the system.

Below we will consider variants of practical use of the proposed focusing versions in the transmission and lidar tomographic systems.

2. Transmission tomography

Figure 2 depicts a schematic layout of the operative experimental radio tomograph. This system measures the complex transfer coefficient of the object under study. This gives the information about the phase and amplitude of radiation having passed through the object.

To measure phase values of the scattered field, the reference and information channels were used. The coming radiation is divided between them with a double waveguide tee. The experimental setup operates in the frequency range of 8–12 GHz. Radiation is focused by two gypsum lenses, each about 32 cm in diameter. The field in the focal zone has an approximately plane phase front and small phase variations along the wave channel.

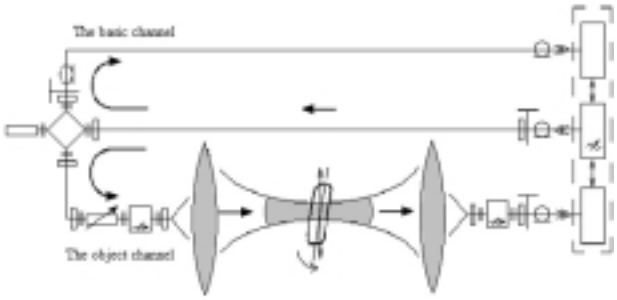

Fig. 2. Layout of transmission radio tomograph.

This setup was used for tomographic scanning of an inhomogeneous test object. The amplitude–phase distribution of wave projections at radio transmission was recorded with a Model R4-36 meter of a complex transfer coefficient. Calibration was carried out with the object removed from the wave channel. The real measurement accuracy was estimated as ± 1 dB in the level and ± 5° in the phase.

To obtain many-angle wave projections of the test object, it was moved linearly and rotated about the working zone of the wave channel. For this purpose, the object was placed on a full-revolving platform with electrical control that provided for precision rotations through the angle θ and motion along one coordinate y.

The experimental data processing was consisted in removing the wave spread of the shadow projections through the deconvolution operation along with the discrepancy functional minimization. This operation, commonly known in the image processing theory, was performed with the use of the Fourier transform and Wiener filtering with regularization.[7,8] To perform it, we must know the instrumental function $Q(\boldsymbol{\rho})$. The shape of this complex function can be refined with the help of a small test object. Somehow or other, deconvolution yields the function $f(\boldsymbol{\rho}_0) = \exp\left\{ik\int \Delta n\left(\mathbf{r}_0'\right)\mathrm{d}z'\right\}$ entering in the integral in Eq. (1). The reconstructed parameter of the exponential function reduces the problem of radio wave (diffraction) tomography formulated here to the well-known problem of X-ray tomography with inversion of the Radon transformation.[1]

The operation of inverse Radon transformation was performed using the well-known Fourier synthesis method.[1] The linear interpolation of the spectrum of spatial frequencies of the object from the polar coordinate system to the Cartesian one was applied. The data processing algorithm was implemented in Mathcad. The experimental data processed in such a way are shown in Fig. 3.

Here we can see a spatial distribution of the object permittivity ($\Delta\varepsilon = 2\Delta n$) relative to its value in a free space. The results obtained agree well with the shape and geometrical dimensions of the test body. With the mean wavelength of 3 cm, the resolution of details of the test object can be estimated as 1 cm.

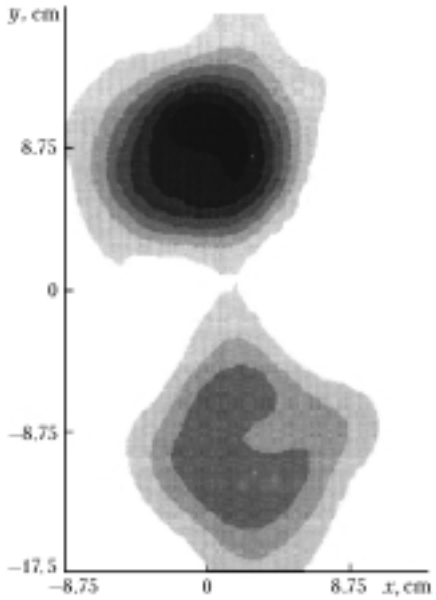

Fig. 3. Transmission tomogram of the test object.

3. Lidar tomography

To conduct test experiments by the lidar tomographic scheme, a wooden box with the dimensions 1.1×1.1×0.9 m was made. On the inside, the box was covered with an absorbing material and filled with sand to the depth of 0.5 m. As a test object, we used a specially made foam polystyrene (foam plastic) step-shaped object with the total size of 15 cm and each step of 5 cm in size. The object was immersed in sand to the depth of 11.5 cm. For sensing we employed the bistatic lidar scheme. The antennas were spaced by $d = 14$ cm. For frequency scanning, the Vector Network Analyzer made by Rohde & Schwarz was applied. We used the range from 2 to 4 GHz, in which the antennas had the standing-wave factor no higher than 1.2. The dynamic range for measurement of signals was about 60 dB.

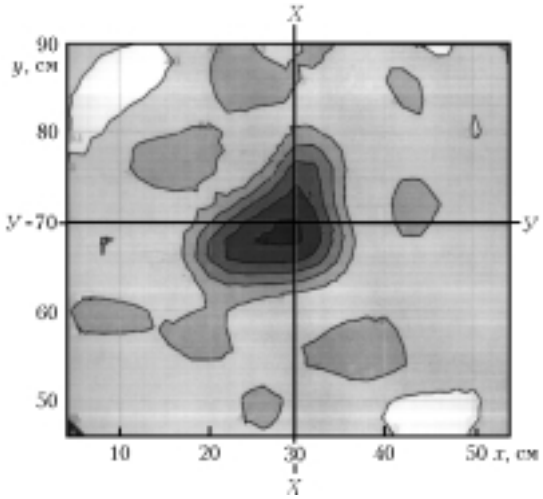

Fig. 4. Lidar tomogram of the test object.

The spatial scanning with the measuring system in two orthogonal directions in the plane lying 30 cm above the media interface with the scanning step of 2 cm yielded a multidimensional spatial-frequency data array consisting of 26×23×256 = 153088 complex readouts. Just this array was initial for tomography.

The data were processed by the algorithm described above. Figure 4 depicts the cross section of the tomogram obtained at the level of location of the test object.

The comparison of the shape of the real object and its tomogram suggests that the resolution achieved is about 3 cm.

The further improvement of the resolution is possible due to extending the frequency range or using pulsed radiation with the pulse duration of about 100 ps and shorter.

Conclusion

Based on experimental investigations with the use of two sensing schemes (in the transmitted and reflected light) the high utility of the focusing effect for radio tomography of inhomogeneous media has been demonstrated. In this case, the influence of multiple interactions decreases significantly and the resolution increases.

Development of the efficient radio tomography methods will allow creation of ecologically safe and relatively cheap diagnostic facilities for medicine and defectoscopy that may be highly competitive to the X-ray tomography. The original approach considered can be used in the development of optical and ultrasonic tomography.

The further promises for improving the informativeness of radio tomography are connected with the use of the ultrabroadband short-pulse radio radiation. This will provide for deeper penetration of radiation and improve the resolution.

Acknowledgments

The support from the Russian Foundation for Basic Research (Grant No. 01–02–17233–a) and the Magdeburg University (Germany) is acknowledged.

References

1. G.A. Fedorov and S.A. Tereshchenko, *Computational Emission Tomography* (Energoatomizdat, Moscow, 1990), 184 pp.
2. V.P. Yakubov, M.L. Masharuev, S.A. Slavgorodskii, D.V. Losev, and S.E. Shipilov, Atmos. Oceanic Opt. **10**, No. 12, 942–946 (1997).
3. Yu.A. Eremin, V.I. Ivanenko, and M.V. Ryazanov, Radiotekhn. Elektron. **43**, No. 2, 133–143 (1998).
4. V.P. Yakubov and M.L. Masharuev, Microwave and Optical Technology Letters **13**, No. 4, 187–189 (1996).
5. V.P. Yakubov and M.L. Masharuev, Izv. Vyssh. Uchebn. Zaved., Fiz., No. 4, 87–92 (1997).
6. V.E. Zuev, V.A. Banakh, and V.V. Pokasov, *Modern Problems of Atmospheric Optics*. Vol. 5. *Optics of the Turbulent Atmosphere* (Gidrometeoizdat, Leningrad, 1988), 370 pp.
7. A.N. Tikhonov and V.Ya. Arsenin, *Methods for Solution of Ill-Posed Problems* (Nauka, Moscow, 1979), 288 pp.
8. G.I. Vasilenko and A.M. Taratorin, *Image Reconstruction* (Radio i Svyaz', Moscow, 1986), 304 pp.